J. Synchrotron Rad. (1999). **6**, 29–33

High-resolution synchrotron radiation Renninger scan to examine hybrid reflections in InGaP/GaAs(001)

M. A. Hayashi,[a]* L. H. Avanci,[a] L. P. Cardoso,[a] J. Bettini,[a] M. M. G. de Carvalho,[a] S. L. Morelhão[b] and S. P. Collins[c]

[a]Instituto de Física 'Gleb Wataghin', UNICAMP, CP6165, 13083-970, Campinas, SP, Brazil, [b]Instituto de Física, Universidade de São Paulo, CP 66318, 05315-970, São Paulo, SP, Brazil, and [c]CLRC Daresbury Laboratory, Warrington WA4 4AD, UK. E-mail: hayashi@ifi.unicamp.br

(*Received 9 June 1998; accepted 6 October 1998*)

High-resolution synchrotron radiation Renninger scans (RS) have been used in the analysis of hybrid reflections in the InGaP/GaAs structure. Four-beam cases involving two Bragg (primary and secondary) and one Laue (secondary) reflections of the 002 Renninger scans for the GaAs substrate and the InGaP layer were analysed in detail. Different structures of asymmetry regarding the in-plane directions [110] and $[1\bar{1}0]$ were observed from the measurements of the same three families of four-beam cases, $\{1\bar{1}\}\bar{1}/\{1\bar{1}\}3$, $\{20\}0/\{20\}2$ and $\{3\bar{1}\}\bar{1}/\{3\bar{1}\}3$, at several φ positions. The comparison between the experimental and *MULTX* simulated scan clearly shows a marked asymmetry observed on the $\{20\}0/\{20\}2$ contributions. An asymmetric peak instead of the simulated dip appears due to the layer Laue secondary beam $\{20\}0$ crossing the layer/substrate interface to generate a hybrid peak. The break in the lattice coherence for this heterostructure is shown by the occurrence of an unexpected dip in the layer RS, which does not obey the mirror symmetry.

Keywords: X-ray multiple diffraction; Renninger scans; hybrid reflections; heteroepitaxial structures; lattice coherence.

1. Introduction

The characterization of semiconductor materials is usually performed by double-crystal X-ray rocking-curve, triple-crystal diffractometry and transmission electron microscopy (TEM) measurements, due to the important complementary information which can be obtained from these techniques. However, an alternative approach, whereby the diffraction condition is simultaneously satisfied by two or more atomic planes inside the crystal, can offer several advantages. X-ray multiple diffraction (MD) (Chang, 1984) can add an extra angular dimension to the two-beam rocking-curve diffraction process. Moreover, information obtained from the MD peak profile by Colella (1974), Post (1977, 1979), Chang (1982) and recently Weckert & Hummer (1997) has provided important contributions to the solution of the phase problem. The sample acts as its own highly perfect analyser crystal and eventually the monochromator is not necessary. The crystalline quality can be easily checked at the sample surface or at the layer/substrate interface, without removal of the layer and avoiding complicated procedures for sample preparation as in TEM.

MD arises when an incident beam simultaneously satisfies the Bragg law for more than one set of lattice planes within a crystal. A set of planes called primary (h_p, k_p, l_p), usually parallel to the sample surface, is aligned to diffract the incident beam. The sample is then rotated (φ axis) around the primary reciprocal lattice vector, and several secondary planes (h_s, k_s, l_s) with arbitrary orientation also diffract. A coupling reflection (h_p–h_s, k_p–k_s, l_p–l_s) is responsible for intensity transfer between the primary and the secondary reflections. The record of $I_{\rm primary}$ *versus* φ is called a Renninger scan (RS) (Renninger, 1937) and it shows peaks if the phases associated with the interaction between the primary and the secondary beams constructively interfere, or dips in the converse case. The RS shows symmetry mirrors related to the primary vector symmetry and to the φ rotation (entrance and exit of a reciprocal lattice point from the Ewald sphere) which are very sensitive to small changes in the crystalline lattice.

In epitaxic systems under MD conditions, the interaction between the wave fields from the layer and the substrate lattices generates extra peaks, called hybrid reflections (Morelhão *et al.*, 1991), in the layer or substrate RS. Recently, Sasaki *et al.* (1996*a*, 1997) reported the analysis of the lattice coherence of an InGaAs/AlGaInAs epitaxic layer on InP(001) based on the information obtained from the synchrotron radiation RS. Furthermore, with regard to the position and intensity of the RS peaks, two programs have been developed and successfully tested: (i) *MULTX*, by Salles da Costa *et al.* (1992), which uses the theory of X-ray MD for mosaic crystals and the multiply diffracted intensities are calculated step by step as a function of the φ

angle. The program is based on the iterative method of Parente & Caticha-Ellis (1974) that uses the general term of the Taylor series, and allows for many-beam interactions to be simultaneously considered. *MULTX* has been implemented to simulate synchrotron radiation RS (Sasaki *et al.*, 1996*b*) accounting for the σ polarization of the synchrotron radiation beam (perpendicular to the primary incidence plane) as well as the diffracted-beam path length for thin epilayered materials. It should be pointed out that in high-crystalline-quality materials the path length for high-intensity polarized beams depends strongly on the absorption coefficient. (ii) The program developed by Morelhão & Cardoso (1992) which adjusts the peak position with respect to the symmetry mirrors and its profile, including the hybrid peaks, in the RS. These developments have lead to new results in the analysis of structural (Morelhão & Cardoso, 1993*a*) and mechanical (Morelhão & Cardoso, 1993*b*) properties of epilayered materials.

Four-beam cases, that comprise the incident 000 beam, two Bragg reflected beams (primary and secondary) and one Laue transmitted beam (secondary), are available in the RS. Since they always appear coupled as shown in Fig. 1, information on lattice coherence for both lattices, layer and substrate can be obtained *via* hybrid reflections, if they are observed. As far as we know, MD hybrid reflections in four-beam cases have not been observed in ternary epitaxic systems. In this paper we describe observations of these hybrids by measuring four-beam Bragg–Laue cases of bulk, substrate and layer using the high-resolution RS set-up at station 16.3 of the Synchrotron Radiation Source, Daresbury Laboratory, Warrington, UK. Once these hybrids are observed, they should allow us to obtain structural information related to the lattice coherence of the InGaP/GaAs(001) epitaxic structure.

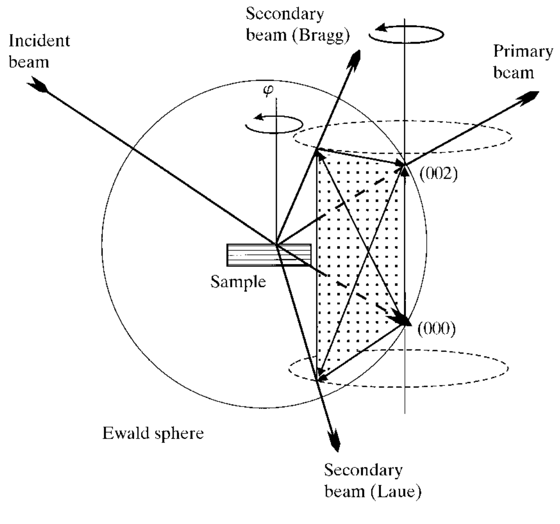

Figure 1
Representation of an MD four-beam case. The primary and one secondary beam are reflected (Bragg) by the sample and the other secondary beam is transmitted (Laue) through the sample.

2. Experimental

High-resolution RS were carried out during the commissioning of the new SRS station 16.3, using 002 as the primary reflection for both the GaAs substrate and the InGaP layer. This station is sited 32 m from a 6 T superconducting wavelength shifter. Highly collimated unfocused X-rays are monochromated by an Si(111) water-cooled channel-cut crystal to provide a tunable ($\lambda \simeq$ 1.4878 Å in this case) beam at the sample position. Goniometry is provided by a large vertically scattering three-axis diffractometer, incorporating a Huber 512 Eulerian cradle, which was designed and constructed at Daresbury for high-resolution X-ray diffraction (Collins *et al.*, 1998). The φ axis enables RS to be performed with a minimum step size of 0.0004° and accuracy less than 0.008°. Due to the intrinsic accuracy of the diffractometer, no special sample alignment is required. The procedure for performing Renninger scans was as follows. First, the sample was mounted with the primary lattice vector nominally parallel to the φ axis. Using calculations based on Busing & Levy (1967), it is then straightforward, after centring the primary reflection, to compute the adjustments to be applied to χ and ω in order to rotate about φ while remaining in the diffracting condition. Typically, such a procedure will fail for an RS due to the smallest of errors in the ω and χ zero angles. To overcome this problem, we measure the ω settings for φ = 0, 90, 180 and 270°, and use these to calculate the ω and χ zeros that will force the correct result at two points, and allow an RS to be performed with minimal errors. This procedure allows very rapid sample alignment, and can give almost constant two-beam diffraction intensities through a complete rotation about the scattering vector.

InGaP layers were grown on top of GaAs(001) substrates by chemical beam epitaxy (CBE) in a Riber MOMBE/CBE system using trimethylindium (TMI), trimethylgallium (TMGa) and phosphine (PH_3) as sources. PH_3 was cracked at 1323 K to provide P and P_2. The layers were grown at 5623 K with a TEGa flow of 1.1 sccm, PH_3 fixed at 10 sccm and the TMIn flow varying from 0.18 sccm to 0.61 sccm (sccm = standard cubic centimetres per minute).

3. Results

The three families of four-beam cases, involving a Laue/Bragg couple in all cases, $\{1\bar{1}\}\bar{1}/\{1\bar{1}\}3$, $\{20\}0/\{20\}2$ and $\{3\bar{1}\}\bar{1}/\{3\bar{1}\}3$, occur in short regions of the RS, spanning less than 1° ($\Delta\varphi < 1°$). They were measured at the regions near φ = 30, 60, 120 and 150°. Fig. 2 shows the regions close to 30 and 60° for bulk GaAs, GaAs substrate and InGaP layer. In Fig. 2(*a*), the same portion of the experimental RS for the GaAs bulk and of the simulated RS using the *MULTX* program with Gaussian peaks are depicted for comparison purposes. One can clearly observe the four-beam $\{1\bar{1}\}\bar{1}/\{1\bar{1}\}3$ and $\{3\bar{1}\}\bar{1}/\{3\bar{1}\}3$ peaks while the $\{20\}0/\{20\}2$ contribution, appearing as a dip, is only visible in the inset. The expected mirror symmetry of these regions with respect to the $\varphi = 45^\circ$ position is observed only in the substrate RS. Fig. 2(*b*) shows a peak instead of the simulated dip for the {20}0/{20}2 contribution, which appears due to the occurrence of a hybrid reflection. The 200 layer Laue secondary beam crosses the interface to be scattered by the $\bar{2}02$ substrate coupling planes towards the detector, giving rise to this hybrid. In the layer RS, Fig. 2(*c*), these regions present different structures of asymmetries with respect to the in-plane directions [110] and $[1\bar{1}0]$. The region around $\varphi = 61^\circ$ shows three dips obtained in the *MULTX* simulated layer RS corresponding to the contributions of the three four-beam cases. The measured positive contributions (peaks) stand for three substrate hybrid (SL) reflections in this case. They are generated by the substrate Bragg secondary beams $3\bar{1}3$ 202 $\bar{1}13$ crossing the interface to be scattered by the layer coupling reflections $\bar{2}1\bar{1}$ $\bar{2}00$ $\bar{1}1\bar{1}$. The occurrence of an unexpected dip at 28.82° (marked with an arrow) shows clearly a break in the symmetry of the Renninger scan around the $\varphi = 45^\circ$ mirror, also observed around 135° (not shown). Then, only the symmetry around the 90° mirror is preserved in this case. Any break in the layer/substrate lattice coherence could cause a phase shift in this hybrid interaction, since it will certainly affect the hybrid path. Once there is a measured 0.6° substrate miscut along $[\bar{1}10]$ in our sample, it causes a difference in the path length of the layer secondary beam, when it crosses the interface to be scattered by the substrate coupling planes. This difference could therefore be responsible for the observed phase shift. Furthermore, it is worthwhile to point out that we were able to detect this effect in the layer RS only because the measurements have been performed in a high-resolution configuration with high spatial coherence in both vertical (>6 μm) and horizontal (>2 μm) directions. A detailed study of the substrate miscut as the possible cause for this phase shift is the subject of a forthcoming paper.

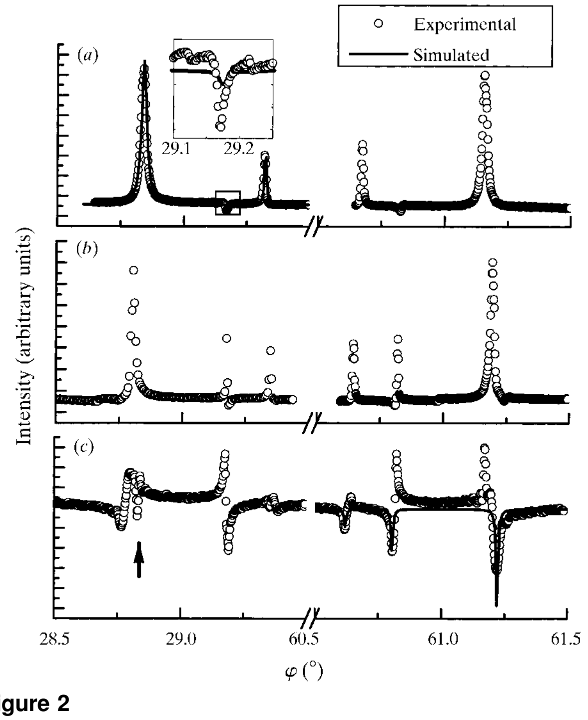

Figure 2
Comparison of the regions around the $\varphi = 45^\circ$ symmetry mirror of the 002 synchrotron radiation RS. (*a*) GaAs bulk with *MULTX* simulation and a magnified view of the {20}0/{20}2 dip in the inset; (*b*) GaAs substrate with the {20}0/{20}2 hybrid layer contribution; (*c*) $In_{0.49}Ga_{0.51}P$ ternary layer with simulation using $a^{\rm layer}$ = 5.6568 Å (from 002 rocking curve). The unexpected dip at 28.82° indicates a change in the phase of this hybrid interaction.

Fig. 3 shows the experimental and simulated 002 rocking curve allowing for the characterization of the tetragonally distorted $In_{0.49}Ga_{0.51}P$ layer with $a_\perp$ = 5.6568 (1) Å and a thickness of 4700 Å. The simulation was obtained using a program based on the Takagi–Taupin equations of X-ray dynamical diffraction (Pesek *et al.*, 1993). The comparison of the rocking curves obtained at each 90° rotation in φ have confirmed that there is no observable tilt between the layer and substrate lattices in the sample. It should be pointed out that the break in the lattice coherence cannot be detected by conventional two-beam X-ray diffraction methods, since the occurrence of two coupled secondary reflections (Bragg and Laue) is required.

Although the $In_{1-x}Ga_xP$/GaAs(001) system can present spontaneous ordering (Kondow *et al.*, 1989; Stringfellow & Chen, 1991) in the $[\bar{1}11]$ and $[1\bar{1}1]$ directions, mainly when $x = 0.50$, we have confirmed that the four-beam cases $\{1\bar{1}\}\bar{1}/\{1\bar{1}\}3$, {20}0/{20}2 and $\{3\bar{1}\}\bar{1}/\{3\bar{1}\}3$, of the RS chosen to be analysed in this work, are not affected by the ordering effect through the MD reflectivity calculation.

In order to fulfill our objective in this work, we have to demonstrate that these four-beam cases in the synchrotron radiation RS are really SL hybrid reflections and thus only the peaks in the layer RS are analysed. Cole *et al.* (1962) proposed a method of indexing the secondary reflections, setting a reference vector perpendicular to the primary one.

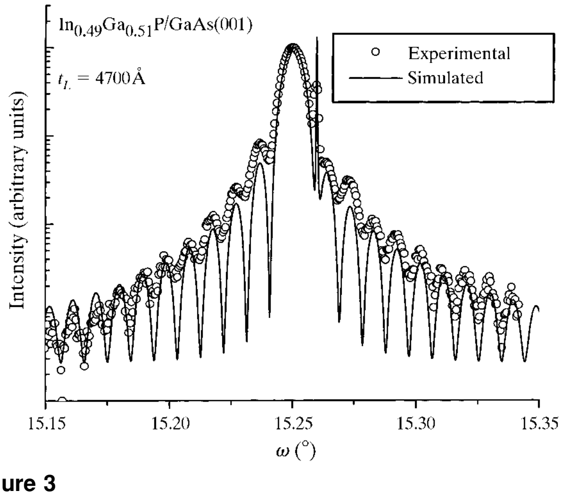

Figure 3
002 rocking curve for the InGaP/GaAs sample using synchrotron radiation, with its simulation.

Table 1

Multiple diffraction (LL) and hybrid (SL) paths and positions around φ = 45° obtained from the layer (InGaP) RS and ω and λ values.

Results considering the two mirrors (45 and 135°) are ω = 15.2389 (19)° and λ = 1.48676 (5) Å.

MD path	$\varphi^{\rm exp}$ (°)	$\varphi^{\rm calc}$ (°)	α (°)	$\beta^{\rm exp}$ (°)	Comments
LL					
$\bar{1}13 + 1\bar{1}\bar{1}$	28.7814	28.7828			
$\bar{1}1\bar{1} + 1\bar{1}3$					
$313 + \bar{3}\bar{1}\bar{1}$	29.3715	29.3724			
$31\bar{1} + \bar{3}\bar{1}3$					
$202 + \bar{2}00$	29.1834	29.1832			
$200 + \bar{2}02$					
SL					
$\bar{1}13_S + 1\bar{1}\bar{1}$	28.8258	28.8262	90	61.1742	ω = 15.2375°
$313_S + \bar{3}\bar{1}\bar{1}$	29.3527	29.3521	−26.5651	55.9178	λ = 1.48672 Å
$202_S + \bar{2}00$	29.1776	29.1740	−45	74.1776	
LL					
$113 + \bar{1}\bar{1}\bar{1}$	61.2206	61.2172			
$11\bar{1} + \bar{1}\bar{1}3$					
$\bar{3}13 + 3\bar{1}\bar{1}$	60.6227	60.6276			
$\bar{3}1\bar{1} + 3\bar{1}3$					
$\bar{2}02 + 200$	60.8146	60.8168			
$\bar{2}00 + 202$					
SL					
$113_S + \bar{1}\bar{1}\bar{1}$	61.1768	61.1738	0	61.1768	ω = 15.2404°
$\bar{3}13_S + 3\bar{1}\bar{1}$	60.6477	60.6479	116.5651	55.9174	λ = 1.48681 Å
$\bar{2}02_S + 200$	60.8232	60.8260	135	74.1768	

Therefore, the φ positions of the MD peaks can be determined in terms of the angle $\beta = \varphi \pm \alpha$, where the +/− signal stands for the in/out positions of the secondary reciprocal lattice point on the Ewald sphere, during the rotation around the primary vector. α is the angle between the secondary vector and the primary incidence plane measured on the Ewald sphere equatorial plane. For a cubic crystal, with $00L$ and hkl as primary and secondary reflections, respectively, β is given by the equation

$$\cos\beta = [(\lambda/2a)(h^2+k^2+l^2) - l\sin\omega]/[(h^2+k^2)^{1/2}\cos\omega],$$

and it is possible to determine both the wavelength (λ) and the incidence angle (ω) by measuring the φ position of two different families of reflections around one symmetry mirror. It should be noted that $\cos\alpha = (h+k)/[2^{1/2}(h^2+k^2)^{1/2}]$ and $\sin\alpha = (-h+k)/[2^{1/2}(h^2+k^2)^{1/2}]$ if the [110] direction is taken as the reference position (φ = 0°) for a (001)-cut crystal. Table 1 gives the calculated and measured angular position of the multiple diffraction (LL) and hybrid (SL) paths around φ = 45°, obtained from the layer (InGaP) Renninger scan. To obtain the ω and λ values (last column), we plotted $\Delta\beta = \beta^{\rm calc} - \beta^{\rm exp}$ over an ω range for the {11}3 and {31}3 reflection of each φ region (45 and 135° mirrors). The experimental ω value is given by the intersection of the two plots and the wavelength λ is obtained adjusting it in order to set the intersection at $\Delta\beta$ = 0. Regarding the two mirrors, the averaged results are ω = 15.2389 (19)° and λ = 1.48676 (5) Å.

It is important to point out the excellent agreement obtained between the calculated and the experimental positions (φ) mainly for the SL hybrid reflections in which the interaction substrate/layer is considered.

4. Conclusions

Here we have observed, for the first time, four-beam hybrid reflections in Renninger scans for ternary epitaxic layers using synchrotron radiation, and their positions were calculated with excellent agreement. These successful observations provide sufficient sensitivity to study lattice coherence of semiconductor structures, provided that the hybrids involve Laue/Bragg coupled secondary reflections from different lattices (layer/substrate), and a highly coherent radiation is employed. Hence, we were able to observe a symmetry break in the hybrid intensity around RS mirrors, which was associated with a change in the path length of the hybrid beam, due to the substrate miscut. This result may have a very important consequence in terms of high-resolution analysis of the layer/substrate interface. The interference of the wave fields has the sensitivity to detect changes in the interface width of the order of the wavelength, and the atomic arrangement (or the coherence) of any semiconductor structure can be investigated with this novel tool. Moreover, the three-dimensional arrangement of such a structure can be achieved by the φ rotation, *i.e.* by measuring the equivalent φ mirrors of a full RS. Therefore, the isomorphism of the growth, with respect to the growth direction, can also be checked.

The authors wish to acknowledge the financial support from the Brazilian Agencies FAPESP, CNPq, CAPES and FAEP/UNICAMP.

References

Busing, W. R. & Levy, H. A. (1967). *Acta Cryst.* **22**, 457–464.
Chang, S. L. (1982). *Phys. Rev. Lett.* **48**, 163–166.

Chang, S. L. (1984). *Multiple Diffraction of X-rays in Crystals*, *Solid State Science Series*, Vol. 50. Berlin: Springer-Verlag.

Cole, H., Chambers, F. W. & Dunn, H. M. (1962). *Acta Cryst.* **15**, 138–144.

Colella, R. (1974). *Acta Cryst.* A**30**, 413–423.

Collins, S. P., Cernik, R. J., Fell, B., Tang, C. C., Harris, N. W., Miller, M. C. & Oszlanyi, G. (1998). *J. Synchrotron Rad.* **5**, 1263–1269.

Kondow, M., Kakibayashi, H., Tanaka, T. & Minagawa, S. (1989). *Phys. Rev. Lett.* **63**, 884–886.

Morelhão, S. L. & Cardoso, L. P. (1992). *Mater. Res. Soc. Symp. Proc.* **262**, 175–180.

Morelhão, S. L. & Cardoso, L. P. (1993*a*). *J. Appl. Phys.* **73**, 4218–4226.

Morelhão, S. L. & Cardoso, L. P. (1993*b*). *Solid State Commun.* **88**, 465–469.

Morelhão, S. L., Cardoso, L. P., Sasaki, J. M. & Carvalho, M. M. G. (1991). *J. Appl. Phys.* **70**, 2589–2593.

Parente, C. B. R. & Caticha-Ellis, S. (1974). *Jpn. J. Appl. Phys.* **13**, 1501–1505.

Pesek, A., Kastler, P., Palmetshofer, L., Hauzenberger, F., Juza, P., Faschinger, W. & Lischka, K. (1993). *J. Phys D*, **26**, A177–180.

Post, B. (1977). *Phys. Rev. Lett.* **39**, 760–763.

Post, B. (1979). *Acta Cryst.* A**35**, 17–21.

Renninger, M. (1937). *Z. Kristallogr.* **106**, 141–176.

Salles da Costa, C. A. B., Cardoso, L. P., Mazzocchi, V. L. & Parente, C. B. R. (1992). *J. Appl. Cryst.* **25**, 366–371.

Sasaki, J. M., Cardoso, L. P., Campos, C., Roberts, K. J., Clark, G. F., Pantos, E. & Sacilotti, M. A. (1996*a*). *J. Appl. Phys.* **79**, 3492–3498.

Sasaki, J. M., Cardoso, L. P., Campos, C., Roberts, K. J., Clark, G. F., Pantos, E. & Sacilotti, M. A. (1996*b*). *J. Appl. Cryst.* **29**, 325–330.

Sasaki, J. M., Cardoso, L. P., Campos, C., Roberts, K. J., Clark, G. F., Pantos, E. & Sacilotti, M. A. (1997). *J. Cryst. Growth*, **172**, 284–290.

Stringfellow, G. B. & Chen, G. S. (1991). *J. Vac. Sci. Technol. B*, **9**(4), 2182–2188.

Weckert, E. & Hummer, K. (1997). *Acta Cryst.* A**53**, 108–143.